Amplification of ultrashort pulses to 0.5 TW at 5 Hz with a flashlamp pumped Cr:LiSAF gain medium

Ricardo E. Samad, Gesse E. C. Nogueira, Sonia L. Baldochi and Nilson D. Vieira Jr

IPEN/CNEN-SP – Centro de Lasers e Aplicações

Av. Prof. Lineu Prestes 2242, 05508-000, São Paulo, SP, Brazil

ABSTRACT

We report here the development and construction of a two-flashlamp pumping cavity for a Cr:LiSAF rod, to be operated as a multipass amplifier in a Chirped Pulse Amplifier system. The pumping cavity was designed to minimize the thermal load on the gain medium by the utilization of intracavity filters, aiming operation with high gain and the highest possible repetition rate. Operating as a laser, 30 Hz repetition rate and 20 W average power were obtained for the first time at a maximum gain per pass of 1.5. Changing the pumping characteristics, the laser provided 16 W at 8 Hz repetition rate, at a maximum gain of 3.6. A four-pass multipass amplifier geometry was designed for the pumping cavity, that was integrated and synchronized to a Ti:Sapphire Chirped Pulse Amplifier system. The amplification properties of the gain medium were determined, in one, two and four passes, along with the gain dependence on the repetition rate. The amplifier final configuration provided amplification by a factor 150 to 20 ps stretched pulses, resulting in final compressed pulses with 60 fs and 0.5 TW of peak power at 5 Hz repetition rate.

Keywords: Cr:LiSAF, CPA, optical amplification, thermal effects, thermal quenching, solid state lasers

1. INTRODUCTION

Single crystals of Cr:LiSAF (Cr^{3+}:$LiSrAlF_6$) show very attractive optical spectroscopic properties[1] for a laser gain medium, such as a long lifetime of the upper laser level (~67μs) at room temperature[2], three broad absorption bands[2] and a wide emission band ranging from 650 nm to 1050 nm. Laser action was demonstrated under several pumping schemes[2, 3, 4, 5], particularly in CW[6] and pulsed regimes. Pulse durations ranging from hundreds of microseconds under free-running pulsed excitation down to nanoseconds in Q-Switching and few femtoseconds in Mode-Locking regime[7] were achieved.

Flashlamp-pumped Cr:LiSAF tunable lasers[3, 8, 9, 10] have been developed reaching pulse energies up to 8.8 J, and flashlamp pumped ultrashort pulse amplifiers[11, 12, 13, 10] reached peak powers up to 8.5 TW. Due to the poor thermal properties of the LiSAF host[14], the operation repetition rate of these lasers/amplifiers were always confined either to the single pulse regime or up to 12 Hz[8]. The low LISAF thermal conductivity leads to crystal cracking due to thermally induced stress, and in the case of a gain medium in the shape of a rod, fracture was observed at 18 Hz[15]. Besides the thermal induced stress that leads to fracture, the lifetime of the Cr:LiSAF laser transition is strongly temperature dependent, dropping from ~67 μs at room temperature to half this value at 69°C, due to thermal quenching[16]. Under flashlamp pumping, the low LiSAF thermal conductivity prevents heat extraction from the laser medium. If the crystal temperature rises above ~25°C, the nonradiactive decay generates more heat, what in turn increases the nonradiactive decay rate, rapidly increasing the crystal temperature. This is a catastrophic process that reduces the energy storage capacity of the crystal and can lead to fracture.

In order to avoid thermal quenching and crystal fracture due to accumulated heat, flashlamp pumped Cr:LiSAF oscillators have been kept operating at low repetition rates. Shimada et al.[8] reported the highest repetition rate and power on a Cr:LiSAF laser to be 4.5 W at 12 Hz, and Perry et al.[17] reported the highest amplifier repetition rate to be 10 Hz for 85 GW pulses. For higher peak powers, Cr:LiSAF amplifiers were always confined to 1 Hz repetition rates or below[10, 11, 12, 13, 18, 19]. Alternatively, a slab geometry laser[9] scheme requires small thickness of the gain medium, allowing

Solid State Lasers XVI: Technology and Devices, edited by Hanna J. Hoffman, Ramesh K. Shori, Norman Hodgson,
Proc. of SPIE Vol. 6451, 645112, (2007) · 0277-786X/07/$15 · doi: 10.1117/12.699130

for better heat extraction and therefore a lower stress in the gain medium and in this case the laser achieved pulse energies as high as 8.8 J, but at 5 Hz repetition rate.

Aiming to raise the repetition rate of flashlamp pumped Cr:LiSAF rod lasers and amplifiers, still keeping its gain and power, we propose a different approach that minimizes the crystal thermal load and temperature gradient by decreasing the heat reaching the gain medium and being generated inside it, by the use of intracavity filters and matching the flashlamps pulse duration to the Cr:LiSAF higher laser level lifetime. To study this scheme, a flashlamp pumped Cr:LiSAF rod pumping cavity was developed and constructed, and initially operated as a laser in a plane concave resonator configuration[20]. The laser could be operated generating 10 kW pulses at 30 Hz and 20 W average power[20], or producing 40 kW pulses at 15 Hz repetition rate and 30 W average power[21] depending on the pumping cavity configuration used. Here we describe some results obtained for the pumping cavity in a multipass amplifier configuration on a hybrid Ti:Sapphire/Cr:LiSAF CPA[22, 23] system, providing a single pass gain over 3 and final pulses of 0.5 TW peak power at 5 Hz repetition rate.

2. PUMPING CAVITY CONCEPTION AND MULTIPASS AMPLIFIER DESIGN

We developed a flashlamp pumped pumping cavity, aiming to minimize the rod thermal load and to increase the operation repetition rate. The rod has a 1.5mol% Cr doping, 101.6 mm of length and 6.35 mm of diameter, with Brewster angled faces. Small diameters allow the extraction of heat more efficiently from the bulk of the rod, decreasing the temperature gradient that leads to rod fracture. The cavity has two 4″ arc-length, 7 mm bore, 450 torr Xenon flashlamps, each one independently fed by a power source capable of delivering up to 50 J in ~67 μs (FWHM) pulses. The power sources were triggered and synchronized to the CPA system by a Stanford Research Systems DG535 delay generator. The flashlamps pulse duration was chosen in order to match the laser transition lifetime, consequently decreasing heat generation by pump energy that is lost to spontaneous emission. The cavity is a closed coupled one, with an alumina diffuse reflector, and cooled by deionized water at 11°C and 30 psi in turbulent flow regime. The humidity in the laboratory is kept under 40%, lowering the dew point, avoiding water condensation on the rod surfaces.

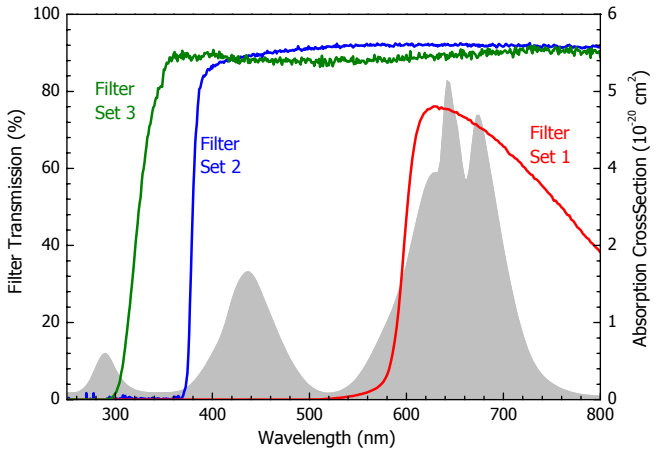

Figure 1. Transmission spectra of the intracavity filters sets used (lines, left scale), and Cr:LiSAF absorption cross section parallel to the c-axis (shaded, right scale).

The temperature of the gain medium inside a pumping cavity is determined by how much energy is absorbed by the medium, and the amount of that energy that is not converted into light emission (spontaneous or stimulated), and how this excess energy is extracted. The main heat source for the Cr:LiSAF crystal is the Stokes-Shift from the three absorption bands centered at 290 nm, 450 nm and 650 nm to the emission band at 830 nm (Figure 1). For a photon absorbed at the center of the 290 nm band resulting in an emitted photon at 830 nm, about 65% of its energy is converted into heat due to the Stokes-Shift. For photons absorbed at the center of the 430 nm and 650 nm bands, these fractions are 50% and 24%, respectively. With the purpose of controlling the heat in the rod, optical filters were inserted

into the pumping cavity between the rod and each one of the flashlamps, selecting the light that is absorbed by the rod and converted into heat in the optical cycle Figure 1. The pumping cavity was designed in a way that the optical filters divide it in three compartments, isolating the rod from the flashlamps, allowing independent coolant flow around each component. The cooling water flows around the rod, and then refrigerates the flashlamps. Thus, heat transfer from the flashlamps to the rod by the cooling water is avoided. In Figure 2 a scheme of the pumping cavity is shown.

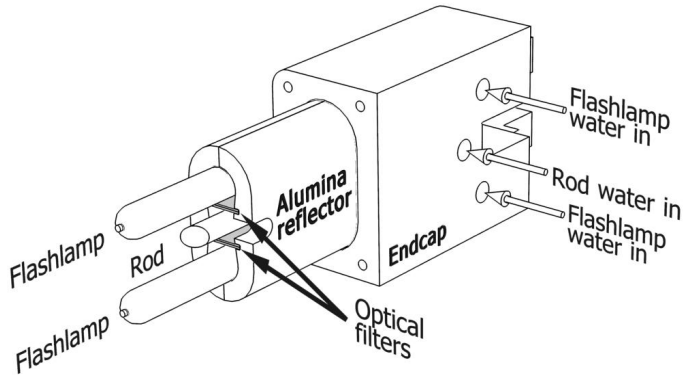

Figure 2. Scheme of the pumping cavity without an endcap. The different cooling water entrances for cooling the crystal and flashlamps are indicated; the optical filters, located between each flashlamp and the crystal, divide the pumping cavity into three independent cooling chambers.

When operating the cavity inside a plane-concave laser resonator, 20 W of average power at 30 Hz repetition rate were extracted whit filter set 1[20], and 30 W at 15 Hz were obtained with filter set 2[21]. Filter set 3 maximizes the thermal effects, decreasing the pulse energy as the repetition rate increases[21], allowing a maximum repetition rate of 8 Hz. Also, this filter set maximizes the excited absorption losses of the gain medium.

To operate as an ultrashort pulse amplifier, the pumping cavity was added to a Ti:Sapphire CPA (Chirped Pulse Amplifier) system. This system comprises a Ti:Sapphire main oscillator (Coherent Mira-Seed) that generates ~20 nm, 50 fs ultrashort pulses, and a Ti:Sapphire multipass amplifier (Quantronix Odin) that stretch, amplify and compress the pulses to ~1 mJ, in ~50 fs FWHM duration.

To amplify the pulses in the Cr:LiSAF pumping cavity developed, after amplification by the Ti:Sapphire, the stretched pulses with $\tau \approx 20$ ps are extracted before the final compressor and injected in the Cr:LiSAF gain medium. We measured the 1-pass amplification for filter sets 1 and 3, and for 2 and 4 passes for filter set 3. Measurements with filter set 2 are being made. A scheme of the 4-passes configuration is shown in Figure 3; for 1-pass amplification measurements, the detector substituted the mirror M_2.

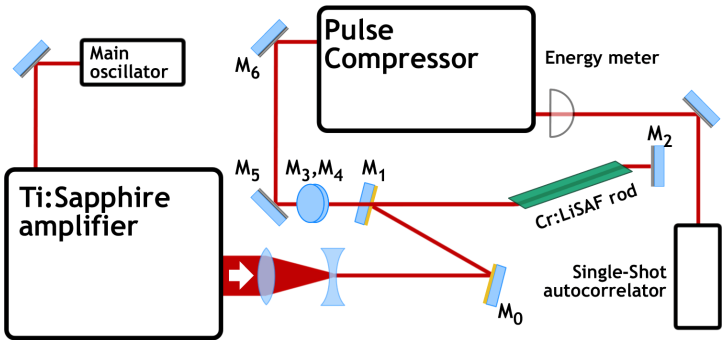

Figure 3. Top view of the hybrid (Ti:Sapphire/Cr:LiSAF) CPA system. After the pulses are stretched and amplified to ~1 mJ inside the Ti:Sapphire amplifier, mirror M_1 injects the pulses into the Cr:LiSAF rod; M_2 reflects the pulses through the rod, above M_1; mirrors M_3 and M_4, in the vertical plane, direct the pulse again to the Cr:LiSAF rod (third pass), and M_2 reflects them to the fourth pass by the rod, to mirrors M_5 and then to the pulse compressor. The energy meter and Single Shot Autocorrelator characterize the pulses.

3. RESULTS

3.1 Filter Set 1 Results

For filter set 1, that pumps the Cr:LiSAF only in the 650 nm absorption band (Figure 1), the 20 ps pulses net amplification measured for each one of the flashlamps individually pumping the gain medium, and for both pumping simultaneously, at 2 Hz repetition rate. The results are shown in Table 1 and Figure 4. From these data we can see that the amplification is the same for each of the flashlamps individually, evidencing that the coupling between each flashlamp and the rod is the same. Since the gain is proportional to the population inversion, that increases linearly with the pumping energy in a 4-level laser system[24] such as the Cr:LiSAF, the amplification was expected to increase exponentially with the pumping energy. The linear dependence observed is du to a small gain regime, which linearizes the amplification dependence. For both flashlamps, this linearization gives amplification below 1 for no pumping, what is incorrect. An exponential fit to these data (dashed line on Figure 4) shows that the discrepancy in the linear fit arises because the linear function is an average of the exponential, and the absence of experimental data near the origin invalidates the approximation on this region

$\mathcal{E}_{pump}$ (J)	Flashlamp 1		Flashlamp 2		Both Flashlamps	
	$\mathcal{E}_{pulse}$ (μJ)	$\mathcal{A}$	$\mathcal{E}_{pulse}$ (μJ)	$\mathcal{A}$	$\mathcal{E}_{pulse}$ (μJ)	$\mathcal{A}$
0	616 ± 12	1	616 ± 12	1	616 ± 12	1
20	650 ± 14	1.055 ± 0.031	651 ± 11	1.057 ± 0.027	668 ± 12	1.084 ± 0.029
40	694 ± 12	1.127 ± 0.029	693 ± 11	1.125 ± 0.028	742 ± 15	1.205 ± 0.034
60	728 ± 14	1.182 ± 0.032	726 ± 13	1.179 ± 0.031	813 ± 16	1.320 ± 0.037
80	768 ± 14	1.247 ± 0.033	765 ± 12	1.242 ± 0.031	875 ± 21	1.421 ± 0.044
100	794 ± 13	1.292 ± 0.033	793 ± 13	1.287 ± 0.033	958 ± 22	1.555 ± 0.047

Table 1. Pumping electric energies ($\mathcal{E}_{pump}$, first column) and Cr:LiSAF rod amplification. In the lamps columns are shown the pulse energies after the rod ($\mathcal{E}_{pulse}$) and the amplification ($\mathcal{A}$) that is the ratio between the pulse energies with and without pumping.

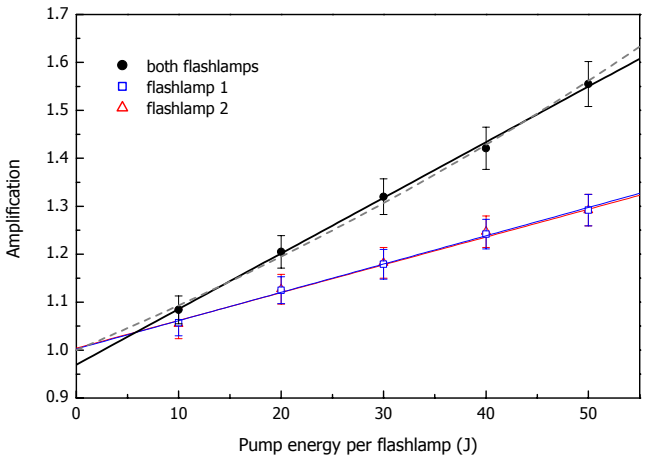

Figure 4. 20 ps pulses amplification by the Cr:LiSAF rod pumped by each flashlamp alone, and by the two flashlamps together, at 2 Hz. The continuous lines are linear functions fitted to the experimental data and the dashed line is an exponential fitted to the two flashlamps pumping data.

The maximum amplification obtained, 1.55 at 100 J total pumping energy, although suitable for a regenerative amplifier, is small for a multipass amplifier as the one that is our objective. That lead us to replace the intracavity filter set 1 by filter set 3.

3.2 Filter Set 3 Results

The filter set 3 single pass amplification results are shown in Table 2 and Figure 5, for 2 Hz repetition rate. In Figure 5 is clearly seen that the amplification grows exponentially with the pumping energy, as expected, indicating a high gain regime. The maximum gain obtained, over 3.6 per pass, suitable for a multipass amplifier.

$\mathcal{E}_{pump}$ (J)	$\mathcal{E}_{pulse}$ (μJ)	$\mathcal{A}$
0	455 ± 8	1.00 ± 0.02
20	582 ± 9	1.28 ± 0.03
40	792 ± 10	1.74 ± 0.04
60	1045 ± 15	2.30 ± 0.05
80	1326 ± 23	2.91 ± 0.07
100	1644 ± 27	3.61 ± 0.09

Table 2. Amplification for 20 ps pulses for filter set 3, at 2 Hz repetition rate.

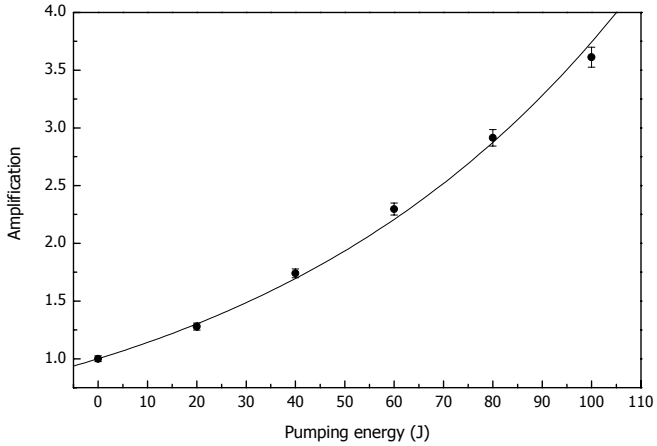

Figure 5. Amplification for 20 ps pulses for filter set 3, at 2 Hz repetition rate, fitted by an exponential function.

The double-pass amplification data is shown in Table 3 and Figure 6, along with the squared single-pass amplification values. The square of the single-pass amplification agrees well with the double pass data, indicating that no additional losses were inserted in the second pass.

$\mathcal{E}_{pump}$ (J)	$\mathcal{E}_{pulse}$ (μJ)	$\mathcal{A}$	$(\mathcal{A}_{1pass})^2$
0	673 ± 8	1.00 ± 0,02	1
20	1088 ± 13	1.62 ± 0,03	1.64
30	1514 ± 14	2.25 ± 0,03	-
40	2040 ± 23	3.03 ± 0,05	3.03
50	2670 ± 26	3.97 ± 0,06	-
60	3430 ± 35	5.10 ± 0,08	5.27
70	4450 ± 46	6.61 ± 0,10	-
80	5950 ± 85	8.84 ± 0,16	8.49
90	8220 ±150	12.21 ± 0,27	-
100	8990 ±430	13.36 ± 0,66	13.05

Table 3. Double pass amplification for 20 ps pulses, at 2 Hz repetition rate. The last column exhibits the square of the single-pass amplification data from Table 2.

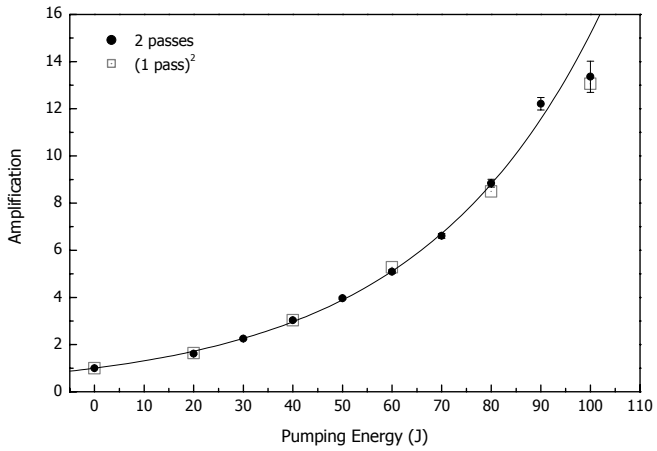

Figure 6. Double pass amplification for 20 ps pulses, at 2 Hz repetition rate, fitted by an exponential function. The squares are the single-pass amplification data squared, showing a good agreement.

In Figure 7 the amplification dependence on the repetition rate is show. This graph exhibits the ration between the amplifications at a given repetition rate and 1 Hz, and we observe that up to 5 Hz the amplification is constant (within the error), dropping for 6 Hz and higher repetition rates. This result is consistent with the behavior observed when operating the pumping cavity as a laser (inside a resonator) with filter set 3[21], and is attributed to thermal effects that diminish the population inversion and consequently decrease the stored energy available to amplify the pulses.

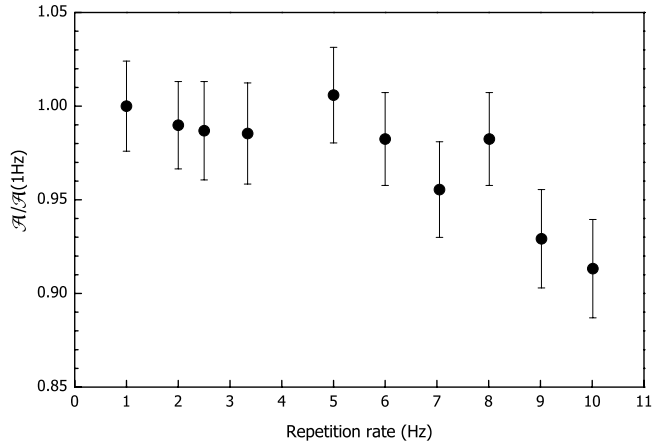

Figure 7. Double-pass amplification dependence on the repetition rate, showing a noticeable drop above 6 Hz.

For the four-pass amplification measurements the scheme shown in Figure 3 was used, at 5 Hz repetition rate, once the amplified pulse energy is the same as at 1 Hz (Figure 7). The data measured is shown in Table 4, Figure 8 (amplification) and Figure 9 (pulse duration). Figure 8 shows the four-pass amplification along with the fourth-power of the single-pass amplification, showing a good agreement except for the last point (100 J pumping); Figure 9 presents the pulse temporal width (FWHM) measured by a single-shot autocorrelator as a function of the pumping energy, and the numerical data, presented in Table 4 fifth column was used to calculate the pulse peak power (Table 4, sixth column); the last point value was not measured, instead it is given by the exponential function fitted to the first five points. The discrepancies on the data at 100 J pumping occur because at this pumping energy the gain medium was damaged by the amplified pulse. This damage occurred at 0.5 TW peak power (last line on Table 4), and after that the amplifier could still be operated at 0.3 TW peak power (second line from the end of Table 4), at an amplification factor above 100 (before the damage the amplification factor measured was above 150). Also, the mirror M_2 was damaged together with

the Cr:LiSAF rod, and measuring the damage size, we estimated a damage threshold of 0.3 J/cm^2 for the mirror. This value is at least one order of magnitude below the usual damage threshold, and together with the damage shape indicate that the beam had hot-spots that locally have very high intensities.

$\mathcal{E}_{pump}$ (J)	$\mathcal{E}_{pulse}$ (μJ)	$\mathcal{A}$	$(\mathcal{A}_{1pass})^4$	τ_p (fs)	P (GW)
0	174 ± 7	1.00 ± 0.06	1	49.9 ± 0.2	3.5 ± 0.1
20	465 ± 13	2.67 ± 0.13	2.69	50.1 ± 0.2	9.3 ± 0.3
40	1535 ± 46	8.82 ± 0.44	9.18	51.0 ± 0.2	30.1 ± 0.9
60	4520 ± 151	26.0 ± 1.4	27.8	53.4 ± 0.2	84.6 ± 2.8
80	11430 ± 350	65.7 ± 3.3	72.1	55.5 ± 0.2	205.9 ± 6.3
100	19000 ± 1000	109 ± 7	170.4	59.8 ± 2	318 ± 16
100	*29650 ± 3000*	*170.4*	*170.4*	*59.8 ± 2*	*496 ± 57*

Table 4. Four-passes amplification data at 5 Hz repetition rate. The fourth column shows the fourth-power of the single-pass amplification, the fifth column exhibits the pulse duration (FWHM) measured by a single-shot autocorrelator, and the last column present the pulses peak power.

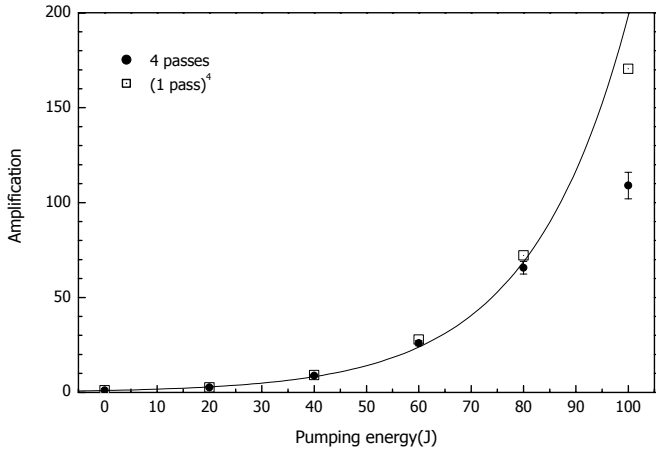

Figure 8. Four-passes amplification data at 5 Hz repetition rate fitted by an exponential function. The squares are the fourth power of the single pass amplification, and the discrepancy at 100 J pumping is due to the rod damage.

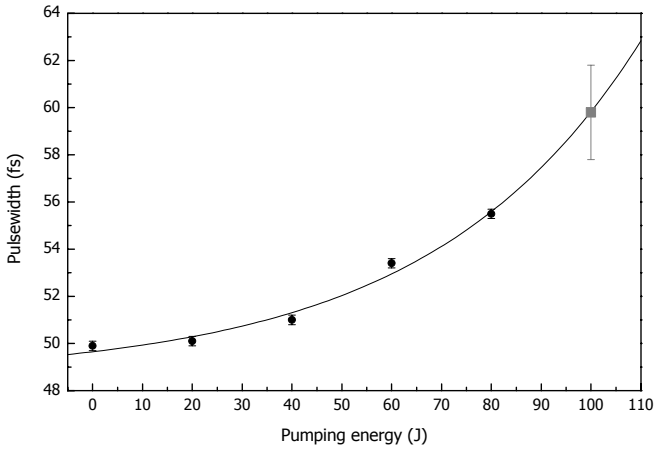

Figure 9. Temporal pulsewidth (FWHM) of the four-passes amplified pulses measured in a single-shot autocorrelator. The 100 J data is extrapolated from the fit to the other data.

The Cr:LiSAF rod was replaced by a new one, and at the moment we are working to improve the beam transversal profile in order to eliminate the hot-spots that damaged it. Also, the intracavity filters were substituted by filter set 3, aiming to minimize thermal effects and decrease the amplification drop with the repetition rate increase keeping the gain almost unchanged, as we observed in the laser[21] configuration. With these changes we expect to obtain TW peak powers at 10 Hz repetition rate.

4. CONCLUSIONS

We developed a Cr:LiSAF pumping cavity with reduced thermal load in the crystal rod, that could be operated as a laser or as an ultrashort pulse amplifier. Amplification over 150 was obtained, resulting in pulses with 0.5 TW of power at 5 Hz repetition rate. At this pulse power the gain medium was damaged as a consequence of the presence of hot-spots in the beam. Even with the damage, the amplifier generated 0.3 TW peak power pulses, at 5 Hz repetition rate. The correction of the beam spatial inhomogeneities will improve the transversal energy distribution allowing amplification to higher energies and peak powers to the 1 TW region, and the use of intracavity filters is expected to allow operation at higher repetition rates.

ACKNOWLEDGEMENTS

The Authors thank Dr. Wagner de Rossi for helpful discussions when designing the pumping cavity and FAPESP for financial support under the grant 00/15135-9.

REFERENCES

1. S. A. Payne, L. L. Chase and G. D. Wilke, "Optical Spectroscopy of the New Laser Materials, $LiSrAlF_6$-Cr^{3+} and $LiCaAlF_6$-Cr^{3+}", *J. of Luminescence* **44**, 167-176 (1989).
2. S. A. Payne, L. L. Chase, L. K. Smith, W. L. Kway and H. W. Newkirk, "Laser Performance of $LiSrAlF_6$:Cr^{3+}", J. *Appl. Phys.* **66**, 1051-1065 (1989).
3. M. Stalder, B. H. T. Chai and M. Bass, "Flashlamp pumped Cr:$LiSrAlF_6$ laser", *Appl. Phys. Lett.* **58**, 216-218 (1991).
4. R. Scheps, J. F. Myers, H. B. Serreze, A. Rosenberg, R. C. Morris and M. Long, "Diode-pumped Cr:$LiSrAlF_6$ laser", *Opt. Lett.* **16**, 820-822 (1991).
5. B. Agate B, A. J. Kemp, C. T. A. Brown and W. Sibbett, "Efficient, high repletion-rate femtosecond blue source using a compact Cr:LiSAF laser", *Opt. Express.* **10**, 824-831 (2002).
6. M. Ihara, M. Tsunekane, N. Taguchi And H. Inaba, "Widely tunable, single-longitudinal-mode, diode pumped CW Cr:LiSAF laser", *Electron Lett.* **31**, 888–889 (1995).
7. S. Uemura and K. Torizuka, "Generation of 12-fs pulses from a diode-pumped Kerr-lens mode-locked Cr:LiSAF laser", *Opt. Lett.* **24**, 780-782 (1999).
8. T. Shimada, J. W. Early, and N. J. Cockroft, "Repetitively pulsed Cr:LiSAF for LIDAR applications", in *OSA Proc. Advanced Solid State Lasers*, 1994, 188–191.
9. D. E. Klimek and A. Mandl, "Power Scaling of a Flashlamp-Pumped Cr:LiSAF Thin-Slab Zig-Zag Laser", IEEE *J. Quantum Elec.* **38**, 1607-1613 (2002).
10. H. Takada, K. Miyazaki and K. Torizuka, "Flashlamp-Pumped Cr:LiSAF Laser Amplifier", *IEEE J. Quantum Elec.* **33**, 2282-2285 (1997).
11. W E. White, J. R. Hunter, L. Van Woerkom, T. Ditmire, and M. D. Perry, "120-fs terawatt Ti:Al_2O_3/Cr:$LiSrAlF_6$ laser system", *Opt. Lett.* **17**, 1067-1069 (1992).

12. Paul Beaud, Martin Richardson, Edward J. Miesak, and Bruce H. T. Chai, "8-TW 90-fs Cr:LiSAF laser", *Opt. Lett.* **18**, 1550-1552 (1993).

13. T. Ditmire, H. Nguyen, and M. D. Perry, "Amplification of femtosecond pulses to 1 J in Cr:$LiSrAlF_6$", *Opt. Lett.* **20**, 1142-1144 (1995).

14. S. A. Payne, L. K. Smith, R. J. Beach, B. H. T. Chai, J. H. Tassano, L. D. DeLoach, W. L. Kway, R. W. Solarz, and W. F. Krupke, "Properties of Cr:$LiSrAlF_6$ crystals for laser operation", *Appl. Opt.* **33**, 5526-5536 (1994).

15. F. Hanson, C. Bendall and P. Poirier, "Gain measurements and average power capabilities of Cr^{3+}:$LiSrAlF_6$", *Opt. Lett.* **18**, 1423-1425 (1993).

16. M. Stalder, M. Bass, and B. H. T. Chai, "Thermal quenching of fluorescence in chromium-doped fluoride laser crystals", *J. Opt. Soc. Am. B* **9**, 2271-2273 (1992).

17. M. D. Perry, D. Strickland, T. Ditmire and F G. Patterson, "Cr:$LiSrAlF_6$ regenerative amplifier", *Opt. Lett.* **17**, 604-606 (1992).

18. T. Ditmire and M. D. Perry, "Terawatt Cr:$LiSrAlF_6$ laser system", *Opt. Lett.* **18**, 426-428 (1993).

19. T. Ditmire, H. Nguyen and M. D. Perry, "Design and performance of a multiterawatt Cr:LiSrAlF6 laser system", *J. Opt. Soc. Am. B* **11**, 580-590 (1994)

20. R. E. Samad, G. E. C. Nogueira, S. L. Baldochi and N. D. Vieira Jr., "Development of a flashlamp-pumped Cr:LiSAF laser operating at 30 Hz", *Appl. Opt.* **45**, 3356-3360 (2006).

21. R. E. Samad, S. L. Baldochi, G. E. Calvo Nogueira, and N. D. Vieira, Jr., "30 W Cr:$LiSrAlF_6$ flashlamp-pumped pulsed laser", *Opt. Lett.* **32**, 50-52 (2007).

22. D. Strickland and G. Mourou, "Compression of Amplified Chirped Optical Pulses", *Opt. Commun.* **56**, 219-221 (1985).

23. M. D. Perry and G. Mourou, "Terawatt to Petawatt Subpicosecond Lasers", Science **264**, 917-924 (1994).

24. W. Koechner, "Solid State Laser Engineering", Springer Series in Optical Sciences Vol. 1, 5th Ed., Springer-Verlag, Heidelberg (1999).